Optical properties of Eu^{3+} activated $Sr_{10}F_2(PO_4)_6$ elaborated by coprecipitation

A. Zounani, D. Zambon and J. C. Cousseins

Laboratoire de Chimie des Solides, URA 444, Université Blaise Pascal et ENSCCF, F-63177 Aubière Cedex (France)

Abstract

The compound $Sr_{10}F_2(PO_4)_6$ was synthesized by coprecipitation at 1200 °C and characterized by X-ray diffraction, thermogravimetric analysis and IR spectroscopy. The Eu^{3+} fluorescence spectra were recorded in this compound using either a tunable dye laser or a nitrogen laser. Whatever the excitation technique, the emission essentially arises from the $^5D_0$ level of the Eu^{3+} ion. The spectroscopic results are discussed in relation to the existence of different crystallographic sites for Eu^{3+} in this host material.

1. Introduction

The apatites with general formula $M_{10}X_2(PO_4)_6$ with M = Ca, Sr, Ba, Pb and X = F, Cl have been extensively investigated because of their optical properties. Indeed, these halophosphates co-activated with Sb^{3+} and Mn^{2+} ions have useful applications in fluorescent lamps. However, it is surprising to note that the activation of these halophosphates by lanthanide ions did not lead to wide investigations in the optical field; ions such as Eu^{3+}, Nd^{3+}, Tb^{3+} and Ce^{3+} have been very little studied [1–5].

Carrying out a program intended for photoluminescence studies of these ions incorporated into the apatite-like phosphates, our attention was first devoted to the optical characterization of $Sr_{10}F_2(PO_4)_6$. For this purpose, the Eu^{3+} ion was chosen because of its local structural probe properties; it is also an active element for the red-emitting phosphors or for laser crystals. In the case of the fluor-apatite compounds, in addition to optical study of the Eu^{3+} ion, it is important to correlate the fluorescence results with the crystallographic data.

This paper deals with the synthesis and the luminescence of $Sr_{10}F_2(PO_4)_6$ activated by Eu^{3+}.

2. Structural background

The crystal structure of the apatite-like compounds is well known [6]. In particular, the fluoro-apatites crystallize in the hexagonal system (space group $P6_3/m$) with two formula units. In the lattice, the M atoms are located on two non-equivalent sites. The M_I atoms (site 4f) lie on the ternary axes and are coordinated by nine oxygen atoms (point symmetry 3) whereas the M_{II} atoms (site 6h) are in a mirror plane and are coordinated by seven atoms: six oxygen and a fluorine atom (point symmetry m). The triangles delimited by these M_{II} atoms (with $z = 1/4$ and $z = 3/4$) are equilateral and on opposite sides. The fluorine atoms lie at the center of these triangles; they are located in channels running along the c-axis.

3. Preparation of $Sr_{10}F_2(PO_4)_6$

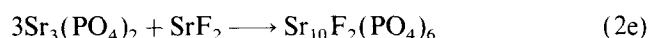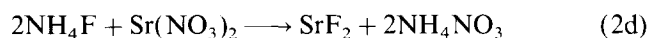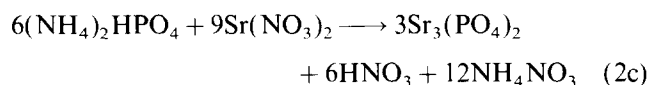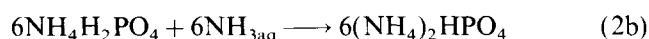The $Sr_{10}F_2(PO_4)_6$ samples were synthesized by coprecipitation. In a first attempt, $Sr(NO_3)_2$, NH_4F and K_3PO_4 were used in aqueous solution as starting materials. The solution containing the F^- and PO_4^{3-} anions was added to the solution containing the Sr^{2+} cation. A gelatinous precipitate was obtained according to the following reaction:

$$10Sr(NO_3)_2 + 2NH_4F + 6K_3PO_4 \cdot 3H_2O \longrightarrow$$

$$Sr_{10}F_2(PO_4)_6 + 18KNO_3 + 2NH_4NO_3 + 18H_2O \quad (1)$$
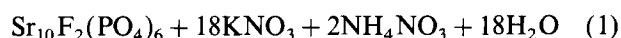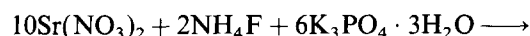
The precipitate was separated from the aqueous solution of potassium and ammonium nitrates, washed, dried in an oven and then fired at 1200 °C under argon flow for 30 min.

H_3PO_4 phosphoric acid in aqueous solution was used as a phosphating agent. In this case, NH_{3aq} was added to the starting solutions of $Sr(NO_3)_2$, NH_4F and H_3PO_4, heated up to 100 °C. As the pH increases, the first H_3PO_4 acidity is neutralized. Immediately after, the pH decreases, owing to the presence of HNO_3. At

this point the apatite starts to precipitate. The reactions are

$$6H_3PO_4 + 6NH_{3aq} \longrightarrow 6NH_4H_2PO_4 \quad (2a)$$

$$6NH_4H_2PO_4 + 6NH_{3aq} \longrightarrow 6(NH_4)_2HPO_4 \quad (2b)$$

$$6(NH_4)_2HPO_4 + 9Sr(NO_3)_2 \longrightarrow 3Sr_3(PO_4)_2$$
$$+ 6HNO_3 + 12NH_4NO_3 \quad (2c)$$

$$2NH_4F + Sr(NO_3)_2 \longrightarrow SrF_2 + 2NH_4NO_3 \quad (2d)$$

$$3Sr_3(PO_4)_2 + SrF_2 \longrightarrow Sr_{10}F_2(PO_4)_6 \quad (2e)$$

$$6HNO_3 + 6NH_{3aq} \longrightarrow 6NH_4NO_3 \quad (2f)$$

The precipitation is complete as the pH reaches neutrality (reaction (2f)). All these reactions take place *in situ* (the intermediate $Sr_3(PO_4)_2$ and SrF_2 are not detected by X-ray analysis). The overall reaction is

$$10Sr(NO_3)_2 + 2NH_4F + 6H_3PO_4 + 18NH_{3aq} \xrightarrow{100\ ^\circ C}$$
$$Sr_{10}F_2(PO_4)_6 + 20NH_4NO_3 \quad (2g)$$
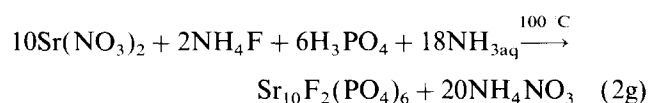
This reaction was carried out at 100 °C in order to improve its rate. The final process for the preparation of $Sr_{10}F_2(PO_4)_6$ was the same as that described when K_3PO_4 was used; the final temperature was also 1200 °C.

4. Characterization of the compounds

The compounds were characterized by X-ray diffraction, thermogravimetric analysis (TGA) and IR spectroscopy.

4.1. X-ray diffraction

The X-ray powder diffraction patterns were recorded with a Siemens D500 diffractometer using $CuK\alpha_1$ radiation ($\lambda = 1.5405$ Å).

After drying the precipitate at 120 °C, the beginning of crystallization of $Sr_{10}F_2(PO_4)_6$ is observed and after calcination at 1200 °C for 1/2 h the X-ray diffraction patterns of the compounds produced according to reactions (1) and (2g) indicate the completion of crystallization. It is worthwhile noting that good crystallinity is already obtained at 700 °C.

The unit cell parameters of $Sr_{10}F_2(PO_4)_6$ synthesized according to reaction (1) are $a = 9.744$ Å, $c = 7.253$ Å; this allows us to consider that a certain amount of OH^- is incorporated into the framework of the fluoro-apatite, which is unfavorable (the cell parameters of $Sr_{10}F_2(PO_4)_6$ and $Sr_{10}(OH)_2(PO_4)_6$ are respectively $a = 9.71$ Å, $c = 7.28$ Å [7] and $a = 9.76$, $c = 7.26$ Å [8]).

However, the unit cell parameters of $Sr_{10}F_2(PO_4)_6$ prepared by reaction (2g) ($a = 9.706$ Å, $c = 7.281$ Å) are similar to those given in ref. 7.

4.2. Thermogravimetric analysis

TGA measurements were taken under argon flow. The results obtained are shown in Fig. 1 for the gelatinous $Sr_{10}F_2(PO_4)_6$ synthesized by the two reaction paths. For the fluoro-apatite elaborated according to reaction (1) (Fig. 1(a)), steps are observed between 100 and 700 °C owing to the loss of H_2O lying on the surface or in the channels [9]. Between 1000 and 1200 °C, a further step is noticed which could be attributed to the evolution of H_2O, according to the following reaction:

$$2OH^- \longrightarrow O^{2-} + H_2O \quad (3)$$

According to Trombe [10], reaction (3) can be reversible. It is due of course to the hydroxy part of the compound.

For $Sr_{10}F_2(PO_4)_6$ prepared according to reaction (2g) (Fig. 1(b)), a plateau is reached at 700 °C; no step is observed between 1000 and 1200 °C. According to Arends et al. [9], a small amount of H_2O evolution can be due to the following reactions:

$$2HPO_4^{2-} \longrightarrow P_2O_7^{4-} + H_2O \quad (4a)$$

$$P_2O_7^{4-} + 2OH^- \longrightarrow 2PO_4^{3-} + H_2O \quad (4b)$$
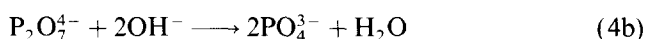
These reactions take place in the ranges 200–550 °C and 700–850 °C. This last step is not observed. This could indicate that the HPO_4^{2-} anions are not present in the jelly apatite framework. The amount present could be very small, but not detectable by thermal analysis.

4.3. IR spectroscopy

The IR spectra were recorded between 4000 and 400 cm⁻¹ using a Fourier-transformed Nicolet type 5SXC spectrometer. The results obtained for the different syntheses are shown in Fig. 2.
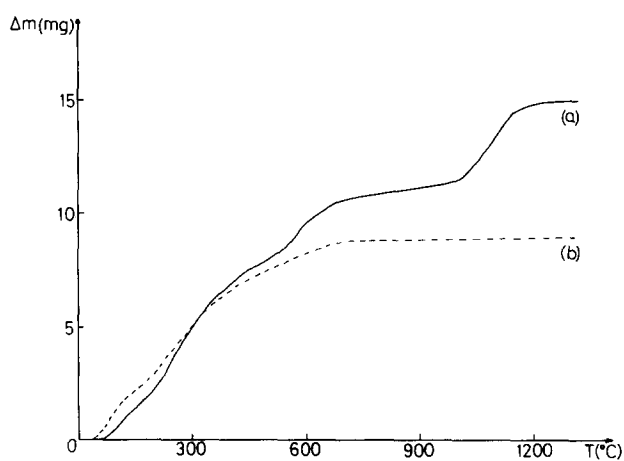

Fig. 1. Thermogravimetric analysis of $Sr_{10}F_2(PO_4)_6$: (a) synthesis by reaction (1), (b) synthesis by reaction (2g).
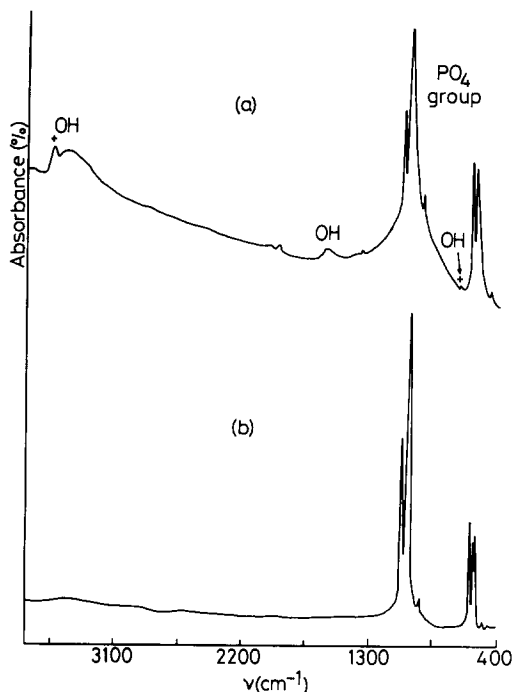
Fig. 2. IR spectra of $Sr_{10}F_2(PO_4)_6$: (a) synthesis by reaction (1) (the lines marked + are characteristic of the hydroxy-apatite), (b) synthesis by reaction (2g).

The IR spectrum of $Sr_{10}F_2(PO_4)_6$ elaborated by reaction (1) (Fig. 2(a)) shows the presence of two broad bands centered at 3470 and 1625 cm^{-1} (OH vibrations); two other narrow bands, near 3550 and 660 cm^{-1}, are characteristic of the OH groups in the hydroxy-apatites [11]. These bands are extremely weak in the IR spectrum of the fluoro-apatite obtained by reaction (2g) (Fig. 2(b)).

The bands between 400 and 1200 cm^{-1} are attributed to the PO_4 groups [12].

All these characterizations allow us to ascertain that preparation of $Sr_{10}F_2(PO_4)_6$ according to the second path (with H_3PO_4) is the best method. Using the first method, solid solution $Sr_{10}F_{2-x}(OH)_x(PO_4)_6$ is obtained. However, the presence of residual H_2O molecules or OH$^-$ ions in interstitial sites or in normal positions is possible even if technique (2g) is used. This could be due to the synthesis method (coprecipitation).

5. Optical measurements

Taking into account the previous results, the compound $Sr_{10-x}Eu_{2x/3}F_2(PO_4)_6$ with $x = 0.15$ ($C = 1\% Eu^{3+}$) was prepared, following the second method, for optical measurements which were performed at 77 K using a tunable dye laser pumped by a nitrogen laser (Jobin Yvon LA O4). Rhodamine 590
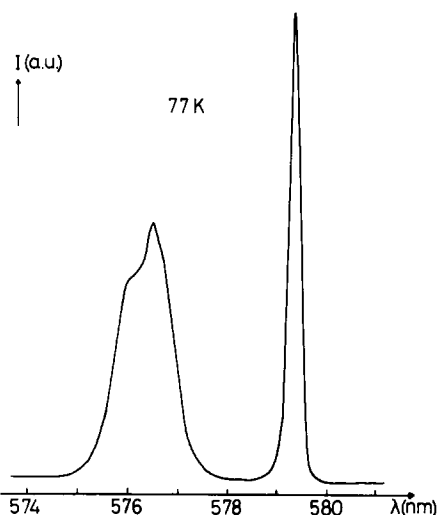

Fig. 3. Excitation spectrum of Eu^{3+} fluorescence emission in $Sr_{10}F_2(PO_4)_6$:1% Eu^{3+} near the $^7F_0 \longrightarrow ^5D_0$ range ($T = 77$ K).

and PBBO for Optilas were used as dyes. The emission was analyzed by a Jobin Yvon HR 1000 monochromator and detected by a Hamamatsu R1104 photomultiplier. The dye signal was filtered through a Boxcar averager PAR model 162/164.

The excitation spectra of Eu^{3+} fluorescence were recorded at 77 K, near the $^7F_0 \longrightarrow ^5D_0$ wavelength range. The result obtained for $Sr_{10}F_2(PO_4)_6$:1% Eu^{3+} is shown in Fig. 3. Three different lines are observed: one of them, lying at 579.4 nm, is narrower than the other two, at 575.9 and 576.4 nm. The narrow line is assumed to correspond to the $^7F_0 \longrightarrow ^5D_0$ transition belonging to one Eu^{3+} site. The two broad lines would indicate the presence of $Eu^{3+}-OH^-(O^{2-})$ ion-coupling, as in $NaYF_4$:Eu^{3+} [13] or the formation of $Eu^{3+}-(F^-)_n$ complexes [14].

The Eu^{3+} emission spectra were recorded at 77 K, upon excitation in the $^5D_0$ and $^5L_6$ levels using the dye laser or at 337.1 nm using the nitrogen laser. The result obtained for $Sr_{10}F_2(PO_4)_6$: 1% Eu^{3+} in the first case is shown in Fig. 4 for excitation at 579.4 nm (Fig. 4(a)) and in the range 575.9–576.4 nm (Fig. 4(b)). The different lines were assigned to the $^5D_0 \rightarrow ^7F_J$ transitions. Their wavelengths and energies are given in Table 1. It is important to note that the lines shown in Fig. 4(b) are narrower than those shown in Fig. 4(a).

With the nitrogen laser or when the $^5L_6$ level is excited, all the emissions are simultaneously observed, those corresponding to Fig. 4(b) being the most intense. Moreover, in this case, transitions arising from the $^5D_2$ or $^5D_1$ levels of the Eu^{3+} ion were not observed. The presence of a charge transfer band at low energy, allowing non-radiative relaxation from the upper levels to $^5D_0$ could explain this feature [15]. It is also possible to consider non-radiative multiphonon relaxation (at
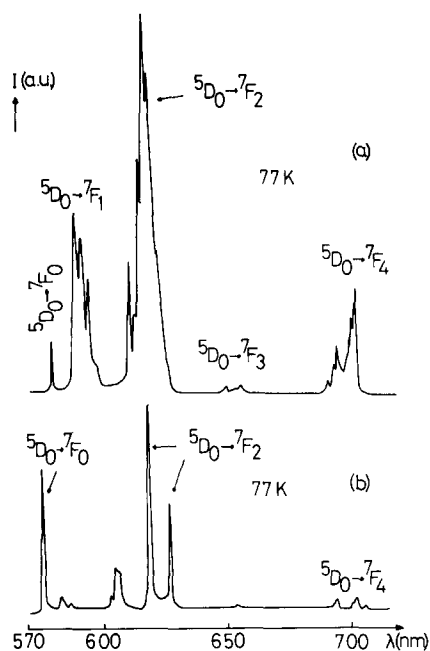
Fig. 4. Fluorescence emission of Eu^{3+} in Sr$_{10}$F$_2$(PO$_4$)$_6$:1% Eu^{3+} at 77 K upon excitation: (a) at 579.4 nm, (b) in the 575.9–576.4 nm range.

present we have no information on the position of the charge transfer state and the cut-off frequency of the phonons).

6. Discussion

The number of lines expected for the $^5D_0 \longrightarrow {}^7F_0$, $^5D_0 \longrightarrow {}^7F_1$ and $^5D_0 \longrightarrow {}^7F_2$ transitions are respectively 1, 2 and 3 under C_3 symmetry and 1, 3 and 5 under C_s symmetry. Taking this into account, it can be argued that the emission shown in Fig. 4(a) corresponds to Eu^{3+} ions incorporated into both C_3 and C_s sites, which could confirm the crystallographic data [6]. Only a single $^5D_0 \rightarrow {}^7F_0$ transition was observed in the emission spectrum (Fig. 4(a)) and in the excitation spectrum (Fig. 3). Two lines corresponding to the $^5D_0 \longrightarrow {}^7F_0$ transitions may be present very close to each other, but they cannot be separated.

Moreover, the most intense lines in Fig. 4(b) appear in the yellow and red–orange ranges. These emissions have been attributed to some Eu^{3+} ions having OH$^-$ or O^{2-} close neighboring ions which are substituting for the F$^-$ ions (the presence of O^{2-} ions is due to a charge balance or to reaction (3)). In this case only the Eu^{3+} ions in the C_s site would be concerned. According to this description, the lines near 576 nm would be attributed to the $^5D_0 \longrightarrow {}^7F_0$ transitions of these Eu^{3+} ions and the lines at 618 and 626 nm to the $^5D_0 \longrightarrow {}^7F_2$ transitions. Moreover, the presence of anions such as

TABLE 1. Wavelengths and energies of the $^5D_0 \longrightarrow {}^7F_J$ transitions

Location of Eu^{3+}	Wavelength (nm)	Energy (cm^{-1})	Assignment
$C_3 + C_s$	579.3	17262	$^5D_0 \longrightarrow {}^7F_0$
	589.6	16961	$^5D_0 \longrightarrow {}^7F_1$
	590.6	16932	$^5D_0 \longrightarrow {}^7F_1$
	591.6	16903	$^5D_0 \longrightarrow {}^7F_1$
	594.4	16824	$^5D_0 \longrightarrow {}^7F_1$
	609.7	16402	$^5D_0 \longrightarrow {}^7F_2$
	610.2	16388	$^5D_0 \longrightarrow {}^7F_2$
	612.6	16324	$^5D_0 \longrightarrow {}^7F_2$
	614.0	16287	$^5D_0 \longrightarrow {}^7F_2$
	616.2	16228	$^5D_0 \longrightarrow {}^7F_2$
	618.0	16181	$^5D_0 \longrightarrow {}^7F_2$
	621.3	16095	$^5D_0 \longrightarrow {}^7F_2$
	650.0	15385	$^5D_0 \longrightarrow {}^7F_3$
	652.6	15323	$^5D_0 \longrightarrow {}^7F_3$
	655.1	15265	$^5D_0 \longrightarrow {}^7F_3$
	687.0	14556	$^5D_0 \longrightarrow {}^7F_4$
	689.2	14510	$^5D_0 \longrightarrow {}^7F_4$
	691.6	14459	$^5D_0 \longrightarrow {}^7F_4$
	694.0	14409	$^5D_0 \longrightarrow {}^7F_4$
	695.0	14388	$^5D_0 \longrightarrow {}^7F_4$
	698.0	14327	$^5D_0 \longrightarrow {}^7F_4$
	700.4	14278	$^5D_0 \longrightarrow {}^7F_4$
	701.3	14259	$^5D_0 \longrightarrow {}^7F_4$
	702.6	14233	$^5D_0 \longrightarrow {}^7F_4$
Eu^{3+}-OH$^-$(O^{2-})	575.2	17385	$^5D_0 \longrightarrow {}^7F_0$
	575.8	17367	$^5D_0 \longrightarrow {}^7F_0$
	582.3	17173	—
	585.8	17071	—
	602.4	16600	—
	605.0	16529	—
	606.0	16502	—
	618.5	16168	$^5D_0 \longrightarrow {}^7F_2$
	626.4	15964	$^5D_0 \longrightarrow {}^7F_2$
	653.5	15302	—
	692.4	14443	$^5D_0 \longrightarrow {}^7F_4$
	693.7	14415	$^5D_0 \longrightarrow {}^7F_4$
	699.4	14298	$^5D_0 \longrightarrow {}^7F_4$
	701.5	14255	$^5D_0 \longrightarrow {}^7F_4$
	706.2	14160	$^5D_0 \longrightarrow {}^7F_4$

O^{2-} or OH$^-$ induces local deformation of the site symmetry. A shift in the energy levels is thus observed. Furthermore, the $^5D_0 \longrightarrow {}^7F_{0,2}$ transitions are sensitive to ligand modification [16, 17]. Thus, all these observations allow us to attribute these lines to Eu^{3+} ions near O^{2-} or OH$^-$ anions.

7. Conclusion

The coprecipitation technique was used successfully for the synthesis of Sr$_{10-x}$Eu$_{2x/3}$F$_2$(PO$_4$)$_6$ ($x = 0.15$, $C = 1\%$ Eu^{3+}). The first results on the fluorescence of Eu^{3+} in this material show that the doping ions are

located in two different crystallographic sites existing in the apatite structure. The emission of Eu^{3+} ions, the environment of which is modified by the presence of OH^- or O^{2-} anions, is also observed.

Our purpose is now to study the concentration ratio dependence of the Eu^{3+} luminescence and to record fluorescence decay in $Sr_{10}F_2(PO_4)_6$. Some measurements have already been recorded and show that the decay values depend strongly upon the synthesis method: they are longer when the compound is elaborated by the coprecipitation technique.

References

1 B. Piriou, D. Fahmi, J. Dexpert-Ghys, A. Taitai and J. L. Lacout, *J. Lumin.*, *39* (1987) 97.

2 F. M. Ryan, R. W. Warren, R. H. Hopkins and J. Murphy, *J. Electrochem. Soc.*, *125* (9) (1978) 1493.

3 J. P. Budin, J. C. Michel and F. Auzel, *J. Appl. Phys.*, *50* (2) (1979) 641.

4 L. H. Brixner and P. E. Bierstedt, *J. Solid State Chem.*, *13* (1975) 24.

5 F. Auzel, J. Dexpert-Ghys, D. Morin, G. Dadoun, J. Ostorero and H. Makram, *Mater. Res. Bull.*, *16* (1981) 1521.

6 J. M. Hughes, M. Cameron and K. D. Crowley, *Am. Miner.*, *74* (1989) 870.

7 E. R. Kreidler and F. A. Hummel, *Am. Miner.*, *55* (1970) 170.

8 G. George, S. K. Gupta, P. V. R. Rao and T. S. B. Narasaraju, *J. Mater. Sci.*, *22* (1987) 2274.

9 J. Arends, J. Christoffersen, M. R. Christoffersen, H. Eckert, B. O. Fowler, J. C. Heughebaert, G. H. Nancollas, J. P. Yesinowski and S. J. Zawacki, *J. Cryst. Growth*, *84* (1987) 515.

10 J. C. Trombe, *Ann. Chim.*, *8* (1973) 251.

11 M. Andres-Verges, F. J. Higes-Rolando and P. F. Gonzales-Diaz, *J. Solid State Chem.*, *43* (1982) 237.

12 W. E. Klee and G. Engel, *J. Inorg. Nucl. Chem.*, *32* (1970) 1837.

13 D. Zakaria, *Thesis*, Clermont-Ferrand, 1991.

14 G. Blasse and A. Bril, *Philips Tech. Rev.*, *31* (1970) 304.

15 C. Delsart, *J. Phys.*, *34* (1973) 711.

16 G. Blasse and A. Bril, *J. Chem. Phys.*, *46* (1967) 2579.

17 W. C. Nieuwpoort and G. Blasse, *Solid State Commun.*, *4* (1966) 227.